A 125–260-GHz Gyrotron

G. FERGUS BRAND, NIGEL G. DOUGLAS, MARK GROSS, JAMES Y. L. MA, LAURENCE C. ROBINSON, AND CHEN ZHIYI

Abstract—**The second gyrotron constructed at the University of Sydney has produced continuous microwave output at more than 60 frequencies in the range 125–260 GHz at power levels approaching 10 W. A gyrotron like this, with broad frequency coverage and moderate power output, has a wide range of possible applications, from spectroscopy to scattering from waves and fluctuations in plasmas.**

In this paper, the results of detailed measurements of frequency, magnetic field, frequency pulling, and starting current are compared with theory. Agreement is excellent. We find that mode conversion at the output end of the cavity determines the level of output power.

I. Introduction

IN THE COURSE of developing a low-power tunable millimeter-wave source for spectroscopy and plasma scattering, two gyrotrons have been constructed at the University of Sydney. Gyrotron I was a fixed-frequency device operating at 120 GHz. Gyrotron II (Fig. 1(a) and (b)), the subject of this paper, was designed to produce a range of frequencies, and has yielded microwave power at levels approaching 10 W from 125 GHz–260 GHz [1].

Performance like this is in marked contrast to that of a gyrotron designed for plasma heating. One recent device [2] delivers high-power (100 kW) pulses at a single frequency (140 GHz).

Gyrotrons such as ours appear to offer higher power and wider tuning than backward-wave oscillators which operate at the same frequencies [3]. Moreover, the problems associated with the manufacture of the intricate slow-wave structure are avoided.

In this paper, the characteristics of Gyrotron II have been studied in considerable detail. Accurate heterodyne techniques have confirmed the frequencies reported in [1], allowed the unambiguous identification of other modes with different azimuthal and axial mode numbers, and enabled an investigation of the frequency pulling (or detuning) which occurs. The experimental results are in excellent agreement with theory.

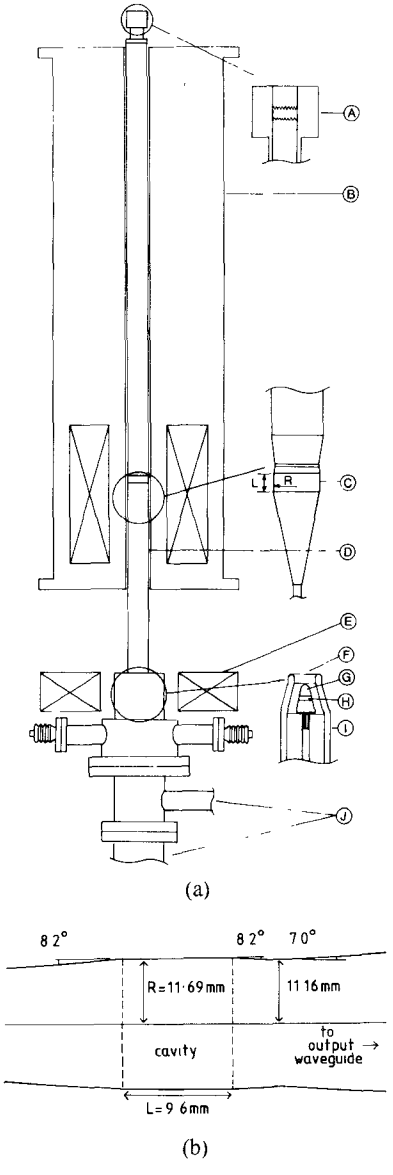

Fig. 1. (a) Gyrotron II. *A* output window, *B* superconducting magnet, *C* resonant cavity, *D* resonator body, *E* auxiliary magnet, *F* electron gun (showing *G* cathode, *H* emitting ring, and *I* anode), and *J* pump ports. (b) The cavity and the transition to the output waveguide in greater detail.

II. Gyrotron II

The magnetron-type electron gun is identical to that used in Gyrotron I [1] and was designed by scaling a Varian gun [4] by a factor of approximately 0.3.

Computer simulations of the electron trajectories show that they are not adequately described by the usual adiabatic theory [5]. Radial electric fields throughout the whole gun region (especially those near the entrance to the resonator body, which are not affected by varying the cathode–anode voltage) contribute to the initial transverse speed of the electrons. Because the magnetic compression ratio in our gyrotron is large, the axial magnetic field in the gun region is small and many electrons leave the gun with such large transverse speeds that they are reflected back.

Manuscript received April 4, 1983; revised August 26, 1983. This work was supported in part by the Australian Research Grants Scheme, the Australian Institute of Nuclear Science and Engineering, the University of Sydney, and the Radio Research Board.

The authors are with the School of Physics, University of Sydney, N.S.W. 2006, Australia.

0018-9480/84/0100-0058$01.00 ©1984 IEEE

These electrons are evidently reflected again in the gun region and have their energy redistributed so that their transverse speed becomes sufficiently low that they can reach the cavity. Some electrons may be reflected many times. We, therefore, expect the mean axial speed in the cavity to be low.

The cavity radius was made large (11.69 mm) so that the modes which are excited would be close together in frequency.

The magnetic field 4.5 to 9.5 T is provided by a superconducting magnet. The cathode emitting ring is 378 mm from the center of the cavity and the magnetic compression ratio $B_{\text{cavity}}/B_{\text{cathode}}$ is 74.0. The distance was chosen so that electrons arriving at the cavity fill an annular ring of approximate mean radius 0.5 mm. This places them very close to inner electric field maxima of all the TE_{0ln} and TE_{1ln} cavity modes in the frequency range, thereby optimizing the gyrotron interaction. (The electrons are too far away from the cavity wall to excite the so-called "whispering gallery" modes.) Operation at the lower frequencies requires an auxiliary magnetic field of ~ 0.04 T at the cathode. This reduces the compression ratio to ~ 50.

The output from the cavity leaves via a long waveguide (radius 13 mm) and passes out of the gyrotron through a wide passband night moth eye quartz window [6].

Two permanent magnets placed just above the superconducting magnet dewar ensure that the electron beam is dumped into the wall of the output waveguide well away from the window.

Typical operating conditions are: cathode–resonator voltage 19.0 kV, anode–resonator voltage 16.5 kV, and beam current 40 mA.

III. Measurements on the Gyrotron Output

Several instruments are available to study the gyrotron output (Fig. 2).

A. Video Detectors

Both *Ka*-band crystal detectors and pyroelectric detectors have been used over the entire frequency range. The former become somewhat insensitive at frequencies above 200 GHz.

B. Fabry–Perot Interferometer

The Fabry–Perot interferometer is used in two configurations: a) with plane-parallel mirrors to measure wavelengths (accuracy ~ 0.3 percent) [7], and b) as a semiconfocal open resonator for high-resolution (better than 2.0 MHz) studies [8]. The displacement of one mirror is controlled by micrometers which are stepper-motor driven over 15 mm. The mirror separation can be made as large as 930 mm.

C. Heterodyne Receiver

The receiver is used to measure frequencies (accuracy better than 10^{-6}). In its original form, it incorporated a *W*-band waveguide-mounted Schottky-diode mixer and a stabilized *X*-band klystron local oscillator. The mixer product is amplified and taken to a spectrum analyzer. Mixing

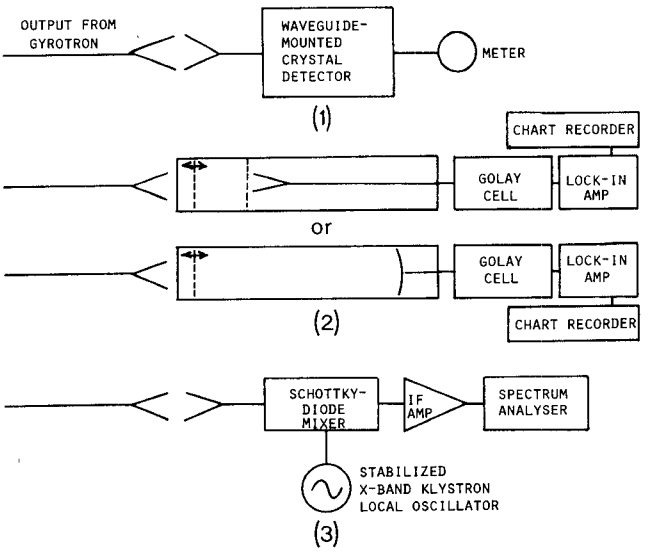

Fig. 2. Arrangement of the instruments used to study the gyrotron output. *1*) Crystal detector, *2*) Fabry–Perot interferometer, and *3*) Heterodyne receiver.

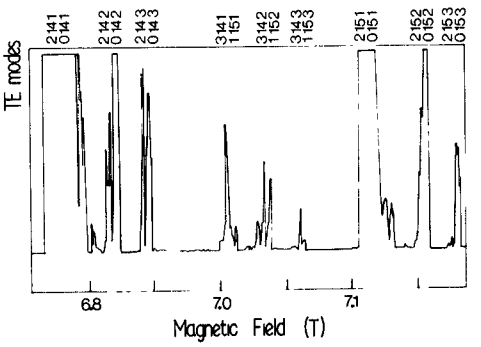

Fig. 3. Signal output versus magnetic field. $V_{\text{cathode-resonator}} = 19.0$ kV, $V_{\text{anode-resonator}} = 16.5$ kV, and $I = 40$ mA.

of the 28th harmonic of the local oscillator with the gyrotron signal has been observed. At higher frequencies, the waveguide-mounted mixer can be replaced by a quasi-optical mixer with a corner reflector.

D. Laser Calorimeter

Power readings from a Scientech Model 36-0001 calorimeter were mutlipled by 1.3 to account for the reduced sensitivity of the device at these wavelengths [7]. Nevertheless, the values are to be taken as a guide only, and are unlikely to be correct to better than ± 30 percent.

Gyrotron II operates continuously. As reported earlier [1], the microwave output over the frequency range is dominated by the TE_{0l1} and TE_{1l1} cavity modes. The original identifications made with the Fabry–Perot interferometer have been confirmed with the receiver (Table Ia). Furthermore, the presence of many other modes has been revealed. A representative group is shown in Table Ib.

Gyrotron II provides a comb of frequencies as the magnetic field is varied (Fig. 3). Measured frequencies are in excellent agreement with the values calculated by applying the method of Vlasov *et al.* [10] to our cavity profile.

The peaks in the gyrotron output come in groups of three. The largest peak is due to the axial number $n = 1$

TABLE Ia
TE_{mln} CAVITY MODES OBSERVED WITH GYROTRON II
(Comparison of calculated and measured values.)

	calc	meas
1 10 1	123.31 GHz	
0 10 1	131.78	131.79
1 11 1	138.12	138.12
0 11 1	144.58	144.59
1 12 1	150.93	150.93
0 12 1	157.39	157.39
1 13 1	163.73	163.76
0 13 1	170.19	170.19
1 14 1	176.55	176.55
0 14 1	182.99	183.00
1 15 1	189.35	189.34
0 15 1	195.80	195.80
1 16 1	202.16	202.15
0 16 1	208.61	208.61
1 17 1	214.97	
0 17 1	221.42	221.45
1 18 1	227.78	227.77
0 18 1	234.23	234.23
1 19 1	240.59	
0 19 1	247.03	
1 20 1	253.40	
0 20 1	259.84	

Note: Axial mode number $n = 1$ modes.

TABLE Ib
TE_{mln} CAVITY MODES OBSERVED WITH GYROTRON II
(Comparison of calculated and measured values.)

	calc	meas
2 14 1	182.81 GHz	182.83 GHz
0 14 1	182.99	183.00
2 14 2	183.87	183.92
0 14 2	184.05	184.10
2 14 3	185.50	185.45
0 14 3	185.68	185.77
2 14 4	187.48	187.48
0 14 4	187.66	187.68
3 14 1	189.00	189.00
1 15 1	189.35	189.34
3 14 2	190.04	190.08
1 15 2	190.39	190.42
3 14 3	191.65	191.73
1 15 3	192.00	192.07
3 14 4	193.62	193.64
1 15 4	193.97	194.00
2 15 1	195.63	195.60
0 15 1	195.80	195.80

Note: All modes observed between TE_{0141} and TE_{0151}.

modes, the TE_{0l1} and nearby TE_{2l1} (or TE_{1l+11} and TE_{3l1}). The azimuthal number 0 and 2 (or 1 and 3) modes are approximately 0.2 GHz (or 0.4 GHz) apart. As the magnetic field is raised, a second smaller and narrower peak appears. This is due to the $n = 2$ modes; TE_{0l2} and TE_{2l2} (or TE_{1l+12} and TE_{3l2}). This is followed by a still smaller peak due to the $n = 3$ modes; TE_{0l3} and TE_{2l3} (or TE_{1l+13} and TE_{3l3}).

Some Fabry–Perot traces show a double structure that suggests the simultaneous occurrence of several modes (Fig. 4). This was difficult to confirm with the heterodyne receiver, so at this point we are not sure if this is genuine multimode operation or a consequence of rapid mode jumping as operating conditions changed slightly due to the small 0.5-percent ripple on the cathode–resonator voltage.

The starting current for the TE_{0141} mode becomes smaller as the magnetic field is increased until it reaches a point where it rises abruptly (Fig. 5).

Frequency pulling was small, of the order of tens of megahertz. Figs. 6–8 show the extent of frequency pulling of the same mode when the magnetic field, cathode–resonator voltage, and anode–resonator voltage were varied.

The bandwidth of the gyrotron signal was small, (1 MHz) (Fig. 9).

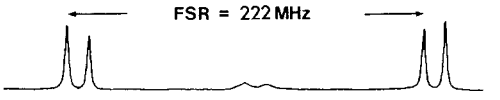

Fig. 4. Fabry–Perot interferometer output showing simultaneous TE_{3141} and TE_{1151} modes. Free spectral range = 222 MHz.

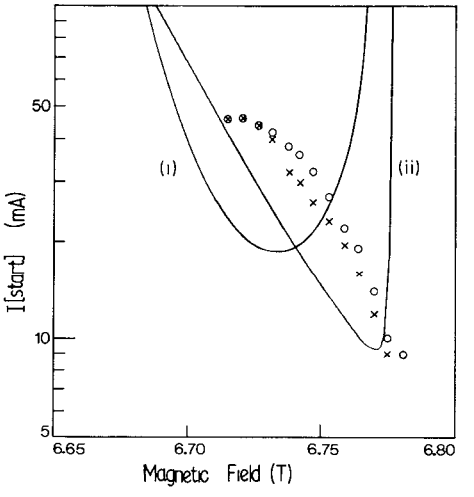

Fig. 5. TE_{0141} mode starting current versus magnetic field. (o: increasing I until output appears, ×: decreasing I until it disappears.) $V_{\text{cathode-resonator}} = 18.8$ kV, $V_{\text{anode-resonator}} = 16.3$ kV. The theoretical curves were calculated for $f = 183.00$ GHz, (*i*) $v_z = 2.0 \times 10^7$ m·s^{-1} and (*ii*) v_z distributed parabolically from 0.1×10^7 to 3.9×10^7 m·s^{-1}, total $Q = 4000$, ohmic $Q = 40000$.

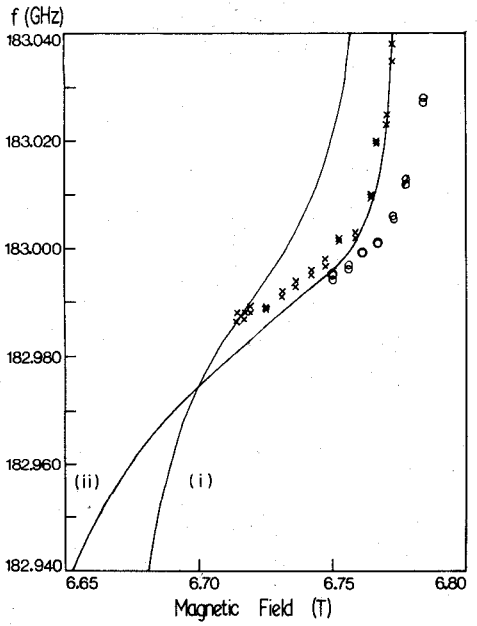

Fig. 6. Frequency of the TE_{0141} mode versus magnetic field. (o increasing B, × decreasing B). In Figs. 6, 7, and 8, except when the quantity was being varied, $B = 6.75$ T, $V_{\text{cathode-resonator}} = 18.8$ kV, $V_{\text{anode-resonator}} = 16.3$ kV and $I = 36$ mA. The theoretical curve was calculated for the same parameters as Fig. 5.

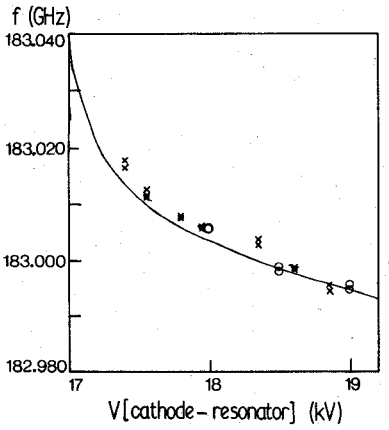

Fig. 7. Frequency versus cathode–resonator voltage.

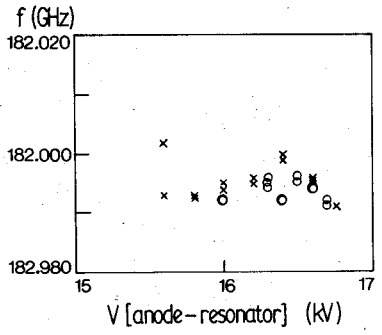

Fig. 8. Frequency versus anode–resonator voltage.

The output power in the strong TE_{0l1} and TE_{1l1} modes measured by the laser calorimeter (and the signal coming out of the crystal detector) was less at the higher frequencies. 5.0 W was measured at 144.59 GHz and 1.5 W was measured at 202.15 GHz. Because of imperfect matching between the output waveguide and the calorimeter, the true power would be greater than these values.

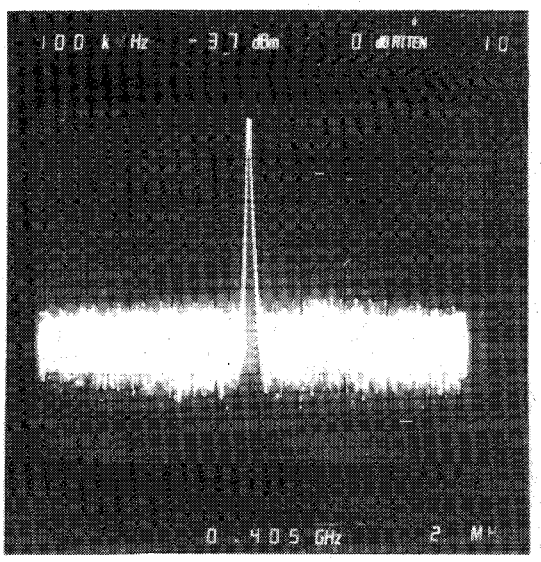

Fig. 9. The gyrotron output as it appears on the spectrum analyzer. Horizontal scale 2 MHz/cm.

IV. Comparison with Theory

The frequencies at which output is observed all correspond to cavity resonances which can be straightforwardly predicted from the dimensions of the cavity. However, the corresponding magnetic fields are given only approximately by equating the wave frequency ω ($= 2\pi f$) and the electron cyclotron frequency Ω ($= eB_{\text{cavity}}/m_0\gamma$, where γ is the relativistic factor). The field for a particular mode is approximately proportional to the frequency, and is lower at low cathode-resonator voltages where the energy of the individual electrons is less (Fig. 10). In order to determine the exact range of magnetic fields over which a particular mode will occur, the conditions for the gyrotron to start must be examined.

Consider the so-called cold electron beam (no spread in momentum variables) where all the guiding centers lie at radius r_0 and the electron orbits are small. The starting current for the fundamental interaction of the beam with the TE_{mln} standing mode in a right-cylindrical cavity is obtained by a small-signal linear analysis of the interaction. It can be written as [11]

$$I_{\text{start}} = -\frac{\pi^3 \epsilon_0 m_0}{e}\frac{\omega v_z^2}{Q}\frac{n^2R^2}{L} \cdot \frac{\left(\xi_{ml}^2 - m^2\right)J_m^2(\xi_{ml})}{\xi_{ml}^2\left[J_{m+1}^2(\xi_{ml}r_0/R) + J_{m-1}^2(\xi_{ml}r_0/R)\right]} \cdot \left[G - \frac{\beta_\perp^2 \Omega}{2kv_z}\frac{dG}{dX}\right]^{-1} \tag{1}$$

where

v_z is the axial electron speed,

$\beta_\perp$ $= v_\perp/c$ where $v_\perp$ is the transverse electron speed,

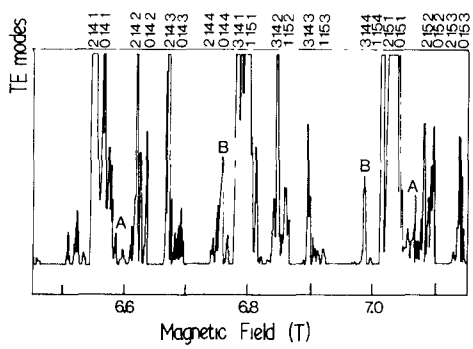

Fig. 10. Signal output versus magnetic field. $V_{\text{cathode-resonator}} = 2.9$ kV, $V_{\text{anode-resonator}} = 1.6$ kV, $I = 80$ mA.

L is the cavity length,
R is the cavity radius,
$k = n\pi/L$,
ξ_{ml} is the lth zero of $J'_m(\xi)$,
Q is the total cavity Q,
$X = (\Omega - \omega)/kv_z$ and
$G = -[(-1)^n \cos n\pi X - 1]/2(X^2 - 1)^2$.

If the beam current I is greater than the starting current, then energy can be transferred to the microwave fields faster than it is being lost as heat to the walls of the cavity or as microwaves down the output waveguide. In general, $I > I_{\text{start}}$ over a range of magnetic fields.

For example, if the beam current is 40 mA, then the starting condition for the TE_{0141} mode at 183.00 GHz will be satisfied at magnetic fields between 6.710–6.775 T. At 6.750 T, the starting current is a minimum 16.8 mA. This calculation assumes a total Q of 4000, a cathode–resonator voltage of 18.8 kV, and $v_z = 2.0 \times 10^7$ m·s^{-1}.

It is difficult to predict the minimum starting current and the magnetic-field range for three reasons. Firstly, the total Q in our gyrotrons is not known. Secondly, neither the axial speed v_z nor the spread in speeds is known precisely. Finally, the microwave electric-field distribution in the cavity is not simply sinusoidal as (1) assumes, but it tails off exponentially in the cutoff regions at either end of the cavity.

However, the groups of three peaks that occur in Fig. 3 can certainly be accounted for qualitatively by applying (1). The starting current is a minimum when the (small-signal) energy transfer is a maximum. This is determined by

$$G - \frac{\beta_\perp^2 \Omega}{2kv_z} \frac{dG}{dX}$$

in (1). Since the second part of this dominates, the energy transfer is greatest where dG/dX is greatest. Fig. 11 shows the magnetic fields where the energies transferred to the TE_{0141}, TE_{0142}, TE_{0143}, and TE_{1151} modes are greatest for different axial speeds. According to Fig. 11(a), the mode with axial number n could be excited at n different magnetic fields [12]. We can use this figure to estimate an axial speed from the spacing of the peaks in the earlier scan (Fig. 3). The separation of the main $n = 2$ and $n = 3$ peaks and

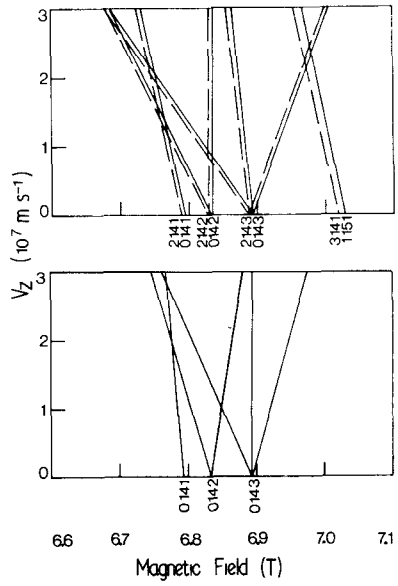

Fig. 11. Magnetic field for maximum energy transfer to several modes for different axial speeds. $V_{\text{cathode-resonator}} = 19$ kV. (a) Calculated for a sinusoidal profile from maxima of dG/dX. (b) Calculated for realistic profile from numerical computation of energy transfer.

the location of the lower field occurrences of the $n = 2$ modes suggests that $v_z < 0.5 \times 10^7$ m·s^{-1}. (Note that the absolute value of the magnetic field is known to ~1 percent. This is not sufficiently accurate to allow us to estimate v_z from the position of the pattern.) The azimuthal number $n = 2$ modes, which lie ~ 0.2 GHz below these, form a similar pattern slightly to the left (broken lines).

If a realistic microwave electric-field profile (obtained in the course of the resonant frequency calculations) is used, instead of the sinusoidal one, the result is the same. Spacing of peaks is sensitive to the profile only at higher axial speeds (Fig. 11(b)).

Under quite different operating conditions (low cathode–resonator voltage 2.9 kV, anode–resonator voltage 1.5 kV, and high-beam current 80 mA), other occurrences of the $n = 2$ and $n = 3$ modes are enhanced (Fig. 10 features labeled A) and $n = 4$ modes appear (B). The spacing of the modes, and hence the estimate of v_z, is the same as before.

The range of fields over which a particular mode occurs is found to become narrower as the beam current is reduced. This is expected from (1).

The starting current results (Fig. 5) show better agreement with theory when a parabolic distribution of axial speeds about 2.0×10^7 m·s^{-1}, rather than a single speed, is assumed. The magnitude of the starting current allows the total Q to be estimated. The low starting currents at the high end of the field range are due to those electrons with very low axial speeds even though there are relatively few of them. They are also responsible for the apparent low axial speed deduced from the scans.

When the same distribution of speeds and total Q are assumed, and the ohmic Q is taken as half of its right cylindrical cavity value, the frequency pulling results (Figs.

6 and 7) show good agreement as well. Note that no points corresponding to the lower half of the curve are present. This is because the starting current exceeds the beam current. The variation with anode–resonator voltage (Fig. 8) is small because radial electric fields near the entrance to the resonator body are at least as important as those between anode and cathode.

So far, no second harmonic operation has been observed. Calculations show that the fundamental starts more easily at most magnetic fields and that the operating current is not quite high enough.

No linear analysis can explain the size and shape of the signals in Figs. 3 and 10. The first peaks generally have a sharp rise on the low magnetic field side and a gradual fall on the high side. The smaller peaks show the opposite behavior.

These features can be predicted by solving the "slow" equations of motion [13] numerically. The result of such a calculation is shown in Fig. 12. The average energy transfer was calculated for a group of 24 electrons with uniformly distributed momentum-space angles. The calculation was carried out for a number of microwave electric-field amplitudes E. The energy transfer is proportional to E^2 only in the small-signal linear regime. At higher values of E, the energy transfer falls off and a point is reached where the energy transferred just equals the energy lost (which remains proportional to E^2). This is the maximum microwave electric field that can be obtained at that particular magnetic field and beam current. The signal escaping from the cavity will be proportional to this. In Fig. 12, this maximum E^2 is plotted as a function of magnetic field for $n=1$ and $n=2$ modes. The sharp rises and gradual falls match the observations.

Agreement with single-mode theory is excellent until the size of the microwave signals is considered. If 10 percent, say, of the power going into the gyrotron is converted into microwave energy in the cavity, then there would be 76 W of microwave power to be shared between ohmic heating losses in the cavity and useful output. The useful output depends on the diffraction Q. Diffraction Q's were obtained in the course of the resonant frequency calculations. They are all very much greater than the ohmic Q's. For example, the diffraction Q for the TE_{0151} mode is $\sim 6\times10^9$ while the theoretical ohmic Q is less than 8×10^4. Under these conditions, a fraction $Q_{\text{ohmic}}/Q_{\text{diffraction}}$ of the power would escape; in this case, less than 1 mW. The observed output is much greater.

The resonant mode is largely trapped in the cavity by the constriction at the output end (Fig. 1(b)). The output power is large because some of the new modes that appear because of mode conversion at the constriction can escape more easily.

A numerical calculation has been carried out for a much simpler case [14] where there is a step from a cavity (radius 11.69 mm) down to an output waveguide (radius 11.16 mm). This shows that if a TE_{015} mode is incident on the step, mode conversion into TE_{016}, TE_{014}, etc. modes does take place. Approximately 30 percent of the power escapes down the narrower waveguide in the TE_{014} mode. Higher radial number l modes remain trapped.

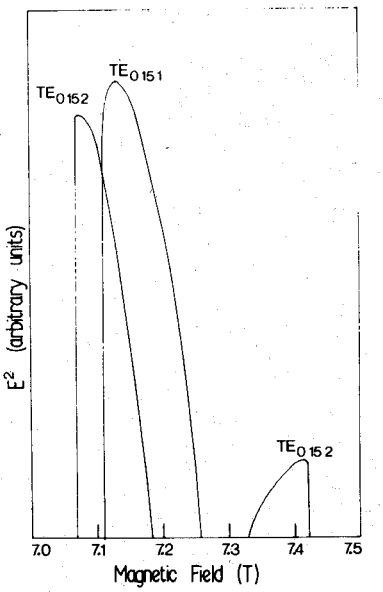

Fig. 12. E^2 versus magnetic field for TE_{0151} and TE_{0152} modes. Note that the vertical scale is different for the two modes. These curves were calculated for $V_{\text{cathode-resonator}} = 20$ kV, $v_z = 3.6\times10^7$ m·s^{-1}, $I = 40$ mA.

This mode conversion is responsible for the low-diffraction Q's and hence the low total Q's that were required earlier to give good agreement between the theory and the observed starting currents and frequency pulling.

References

[1] G. F. Brand, N. G. Douglas, M. Gross, J. Y. L. Ma, L. C. Robinson, and Chen Zhiyi, "Tuneable millimeter-wave gyrotrons," *Int. J. Infrared and Millimeter Waves*, vol. 3, pp. 725–734, 1982.

[2] R. J. Temkin, K. E. Kreischer, W. J. Mulligan, S. MacCabe, and H. R. Fetterman, "A 100 kW, 140 GHz pulsed gyrotron," *Int. J. Infrared and Millimeter Waves*, vol. 3, pp. 427–437, 1982.

[3] G. Kantorowicz and P. Palluel, "Backward wave oscillators," in *Infrared and Millimeter Waves, vol.* 1, K. J. Button, Ed. New York: Academic Press, 1979, pp. 185–212.

[4] H. R. Jory, "Development of gyrotron power sources in the millimeter wavelength range," in *Proc. Joint Varenna-Grenoble Int. Symp. Heating Toroidal Plasmas* (Grenoble, France), July 1978, p. 231.

[5] A. L. Gol'denberg and M. I. Petelin, "The formation of helical electron beams in an adiabatic gun," *Izv. Vyssh. Uchebn. Zaved., Radiofiz.*, vol. 16, pp. 141–149, 1973.

[6] J. Y. L. Ma, M. M. Blanco, and L. C. Robinson, "Night moth eye broadband waveguide window," in *Proc. 7th Int. Conf. Infrared Millimeter Waves* (Marseilles, France), Feb. 1983.

[7] N. G. Douglas and P. A. Krug, "CW laser action in ethyl chloride," *IEEE J. Quantum Electron.*, vol. QE-18, pp. 1409–1410, 1982.

[8] N. G. Douglas, "A high resolution Fabry-Perot interferometer for the millimetre/submillimetre region," in *Proc. 7th Int. Conf. Infrared Millimeter Waves*, (Marseilles, France), Feb. 1983, p. 195.

[9] F. B. Foote, D. T. Hodges, and H. B. Dyson, "Calibration of power and energy meters for the far-infrared/near millimeter wave spectral region," *Int. J. Infrared and Millimeter Waves*, vol. 2, pp. 773–782, 1981.

[10] S. N. Vlasov, G. M. Zhislin, I. M. Orlova, M. I. Petelin, and G. G. Rogacheva, "Irregular waveguides as open resonators," *Izv. Vyssh. Uchebn. Zaved., Radiofiz.*, vol. 12, pp. 1236–1244, 1969.

[11] K. E. Kreischer and R. J. Temkin, "Linear theory of an electron cyclotron maser operating at the fundamental," *Int. J. Infrared and Millimeter Waves*, vol. 1, pp. 195–223, 1980.

[12] K. E. Kreischer and R. J. Temkin, "Mode excitation in a gyrotron operating at the fundamental," *Int. J. Infrared and Millimeter Waves*, vol. 2, pp. 175–196, 1981.
[13] P. Sprangle and A. T. Drobot, "The linear and self-consistent nonlinear theory of the electron cyclotron maser instability," *IEEE Trans. Microwave Theory Tech.*, vol. MTT-25, pp. 528–544, 1977.
[14] F. Sporleder and H.-G. Unger, *Waveguide Tapers Transitions and Couplers*. London: Peter Peregrinus Ltd., 1979, ch. 4.

G. Fergus Brand was born in Dunedin, New Zealand, in 1941. He received the M.Sc. degree from the University of Otago, New Zealand, in 1964, and the Ph.D. degree from the University of Sydney, Australia, in 1968.

Since then, he has worked in the Plasma Physics Department of Sydney University's School of Physics on plasma diagnostics with microwaves, electron cyclotron harmonic wave propagation in reflex discharges, centrifuging of metals in rotating plasmas, and on the development of tunable gyrotrons.

Nigel G. Douglas was born in England in 1955, and received the B.Sc. (Hons.) degree from the University of Sydney, Australia, in 1978. He is currently in the School of Physics, Sydney University, completing the Ph.D. degree, which is particularly concerned with gyrotron instrumentation and applications.

Recently, he worked with the Laser Group at the University of Stuttgart in Germany, investigating pulsed far-infrared systems.

Mark Gross was born in Sydney, Australia, in 1957 and received the B.Sc. (Hons.) degree from the University of Sydney, Australia, in 1980. He is currently completing his Ph.D. degree in the School of Physics, Sydney University where he has played a major engineering role in the design and construction of three low-power, tunable gyrotrons.

James Y. L. Ma was born in Shantou, China, in 1954. He received the B.Sc. degree from the University of Melbourne, Australia, in 1978. Currently, he is completing the Ph.D. degree in the School of Physics, University of Sydney, where his interests are in the development of low-power high-frequency tunable gyrotrons.

Laurence C. Robinson was born in Chiltern, Victoria, Australia, in 1926. He received the M.Sc. degree from the University of Adelaide, Australia, in 1958, and the Ph.D. degree from the University of Sydney, Australia, in 1964.

Since 1962, when he joined the Plasma Physics Department in Sydney University's School of Physics, he has established the microwave plasma diagnostic program and the far-infrared laboratory. This laboratory has developed HCN lasers, rotating mirror and pulsed plasma interferometer diagnostics to monitor electron cyclotron emission from the DITE (U.K.) tokamak and, most recently, low-power tunable gyrotrons. He is the author of the book *Physical Principles of Far-infrared Radiation* (New York: Academic Press, 1973).

Chen Zhiyi was born in Changsha, China, in 1940. He graduated from Chengdu Institute of Radio Engineering, Chengdu, China, in 1962.

Since 1962, when he joined Beijing Vacuum Electron Device Research Institute, China, he has worked on the development and application of the microwave tubes. In recent years, he has been engaged in the research on gyrotrons in China. Since 1982, he has been a Visiting Associate in the University of Sydney, Australia, where he is working on the development of a tunable gyrotron.